MINERALOGICAL COLLECTION
2022. N 72. P. 72–92
ISSN 2078-6220 (print)

МІНЕРАЛОГІЧНИЙ ЗБІРНИК
2022. № 72. С. 72–92
ISSN 2078-6220 (print)

UDC 549:552:551.71(477)

Nataliia Bilyk[1], Iryna Poberezhska[2], Leonid Skakun[3], Yevheniia Slyvko[4]

Ivan Franko National University of Lviv,
4, Hrushevskoho St., Lviv, Ukraine, 79005
[1]nataliya.bilyk@lnu.edu.ua; https://orcid.org/0000-0002-9684-195X
[2]iryna.poberezhska@lnu.edu.ua; https://orcid.org/0000-0001-5020-8326
[3]leonid.skakun@lnu.edu.ua
[4]emslivko@i.ua; https://orcid.org/0000-0002-2731-0602

PECULIARITIES OF THE COMPOSITION AND THERMODYNAMIC CONDITIONS OF FORMATION OF ENDERBITES OF THE HAIVORONSKYI COMPLEX (SOUTH-WESTERN PART OF THE UKRAINIAN SHIELD)

Mineralogical and petrographic features of enderbites of the Haivoronskyi complex in the south-western part of the Ukrainian Shield (the valley of the Pivdennyi Buh River from the town of Haivoron to the village of Zavallia) were studied. The complex of research included field geological observations on outcrops and in quarries and laboratory petrographic, mineralogical and petrogeochemical studies. Such minerals as quartz, plagioclase (albite–oligoclase, andesine–bytownite), K-feldspar (microcline), rhombic (ferrosilite) and monoclinic (diopside, augite) pyroxenes, garnets, biotite, apatite, ilmenite, monazite, carbonates (calcite, dolomite) have been described. The temperature of mineral formation was calculated using garnet-biotite, garnet-orthopyroxene and two-feldspar geothermometers according to the data of various authors using theoretical calculations and a graphic method. The thermodynamic conditions for the formation of enderbites during three stages were determined on the basis of the conducted research and literature data.

Key words: enderbites, mineralogy, petrography, mineralogical geothermometers, Precambrian, Ukrainian Shield.

Introduction. The studied territory is located in the Haivoron district of the Kirovohrad region (Fig. 1) and covers part of the Pivdennyi Buh River valley from the city of Haivoron to the village of Zavallia, geologically – in the south-western part of the Ukrainian Shield, at the junction of two megablocks – Dnistersko-Buzkyi and Rosynsko-Tikytskyi, between which the Holovanivska sutural zone is located.

The geological features of the area within the Dnistersko-Buzkyi megablock are caused by the presence of dome structures composed of rocks of the enderbite complex (U-Pb age of zircon – 3.5–3.3 billion years), and inter-dome depressions filled with carbonate-silicate rocks and complex of ultrabasic (serpentinites, peridotites, pyroxenites) and basic (gabbro) rocks

[10]. The rocks are metamorphosed in the conditions of the granulitic facies. In the Holovanivska sutural zone, dome structures of granitoid composition (age – 1.8 billion years) and inter-dome depressions filled with biotite-amphibole gneisses and crystalline schists (amphibolite facies of metamorphism) are developed; there are relics of the Dnistersko-Buzkyi megablock rocks in some places, which indicates the superimposed character of amphibolitic metamorphism in the sutural zone [10].

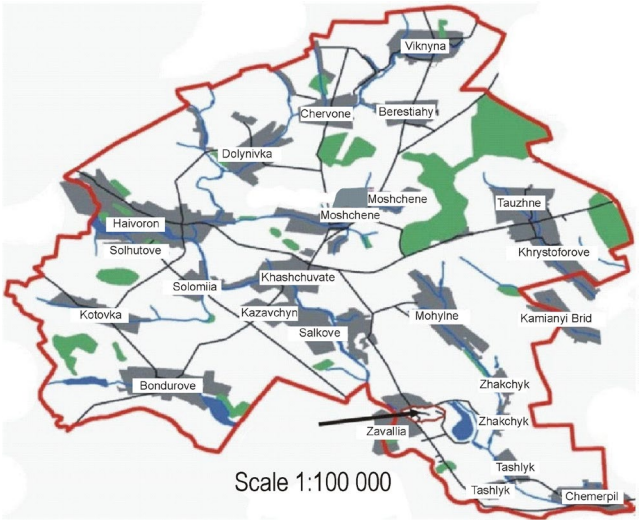

Fig. 1. Overview map of the research area.

The following three structural elements are distinguished in the Middle Pobuzhzhia: the Khashchuvato-Zavallivska synclinal structure (Bilotserkivska tectonic zone), the Pervomaisko-Holovanivska synclinal structure, and the Synytsivska anticlinal structure that separates them (Holovanivska tectonic zone). The Khashchuvato-Zavallivska structure, located between Haivoron and Zavallia, stretches for more than 25 km and is 16 km wide. It is bounded from the south by the Zavallivska fault zone, and from the north – by the Haivoronska fault zone. Two zones are distinguished in the structure: the Khashchuvativska, which is located in the northern part of the structure and has a latitudinal strike (length – 25 km, width – from 0.5 to 3.0 km), and the Zavallivska one in the south-eastern part of the structure (6 × 3 km) [8].

Enderbites are considered the oldest granitoids of the Ukrainian Shield. They are common in the Dnistrovsko-Buzkyi (Haivoronskyi complex), Serednioprydniprovskyi (Slavhorodskyi complex) and Pryazovskyi megablocks (Tokmatskyi complex) [11]. The rocks of the enderbitic formation are exposed most completely and in the most preserved (from the influence of secondary processes) form in the Middle Pobuzhzhia and Transnistria. In some places, the enderbites of the Haivoronskyi complex underwent high-temperature metasomatosis, so it is not always possible to determine which of the potassium feldspars is syngenetic with the enderbites, and which is superimposed.

I. Lesnaia, E. Nalivkina, M. Semenenko, I. Usenko, I. Shcherbakov, H. Yatsenko and other geologists studied the mineral composition of charnockitoids (enderbites).

According to I. Lesnaia [3], the main feature of charnockitoids (enderbites) of the Haivoronskyi block is a layer-like mode of occurrence and a gneiss-like appearance. Among them,

pre-granulitic charnockitoids (they are described in the literature as pre-folded or early-folded, synfolded rocks), or charnockite-migmatites, and late-folded charnockitoids are distinguished.

I. Usenko believed [7] that charnockitoids of the Haivoronskyi complex correspond in composition to enderbites, diorite-enderbites, and plagiocharnockites. They are represented by two-pyroxene and biotite-hypersthene plagiogneisses and crystalline schists, among which the scientist proposed to distinguish rocks of the Haivoronskyi type (two-pyroxene), Yatranskyi type (hypersthene and garnet-hypersthene), and Tokarskyi type (biotite-hypersthene). Potassium feldspars are mainly superimposed, but they are also formed in the conditions of the granulitic facies, which is evidenced by the low ordering of the mineral.

In work [9], the Haivoron-type enderbites, which make up the Haivoron-Zavallivskyi block, are described as greenish-grey very solid rocks. The most leucocratic enderbites contain lenticular lamellar quartz, and the mesocratic enderbites contain cord-like chains of pyroxenes, giving the rocks a stem-like, bundle-like, or cord-like texture. Subparallel allocations are visible in the cross-section.

The following mineral composition of enderbites is given [11]: ortho- and clinopyroxene, garnet, biotite, plagioclase, potash feldspar, quartz. The ratio of minerals is very different, so the composition of the rocks ranges from quartz diorite to trondhjemite. The more basic enderbites are usually bipyroxene, the more acidic ones contain garnet and biotite. Zircon (12–180 g/t), apatite (0–600), and ilmenite (0–300 g/t) prevail among the accessory minerals. Magnetite and monazite appear in rocks with the beginning of potash feldspartization.

Our **goal** is to investigate the peculiarities of the mineral composition of enderbites of the Haivronskyi complex and to characterize the thermodynamic conditions of their formation.

Materials and methods. Mineralogical analysis of enderbite samples, which we selected in the quarries of Kozachyi Yar, Odeskyi, Haivoronskyi, and the northern side of the Zavallivskyi quarry, was performed. The complex of research included field geological observations on outcrops and in quarries and laboratory petrographic, mineralogical and petrogeochemical studies. We studied the mineral composition and structural and textural features of the rocks in transparent sections under the OLYMPUS microscope. Microanalytical studies of polished sections were performed in the laboratory of the Faculty of Physics (Ivan Franko National University of Lviv) using a PEMMA-102-02 (Sumy, Ukraine) raster (scanning) electron microscope equipped with an EDAR energy dispersive analyzer.

Results and discussion. Enderbites are massive medium-coarse-grained grey, dark grey, greenish-grey rocks (Fig. 2). The texture is grano- or heteroblastic. The mineral composition of enderbites is as follows, %: plagioclase – 50, quartz – 10–30, pyroxenes – 15, potassium feldspar – up to 10, garnet – up to 5, biotite – up to 5, hornblende – single grains; less than 1 % are apatite, zircon, titanite, ilmenite, monazite, pyrite, magnetite, calcite, dolomite.

Quartz is represented by isometric or irregular grains 0.1–1.6 mm in size from light to dark grey. Quartz of two generations is available (Fig. 3). Quartz-I forms elongated grains with stylolitic boundaries at the contact with other minerals. Quartz-II was formed as a result of recrystallization and is represented by isometric grains with wavy extinction.

Plagioclase forms tabular grains 1.0–1.5 mm in size, white in colour with characteristic polysynthetic twins (Fig. 4).

The chemical composition of plagioclase according to the results of microprobe analysis is given in Tables 1 and 2.

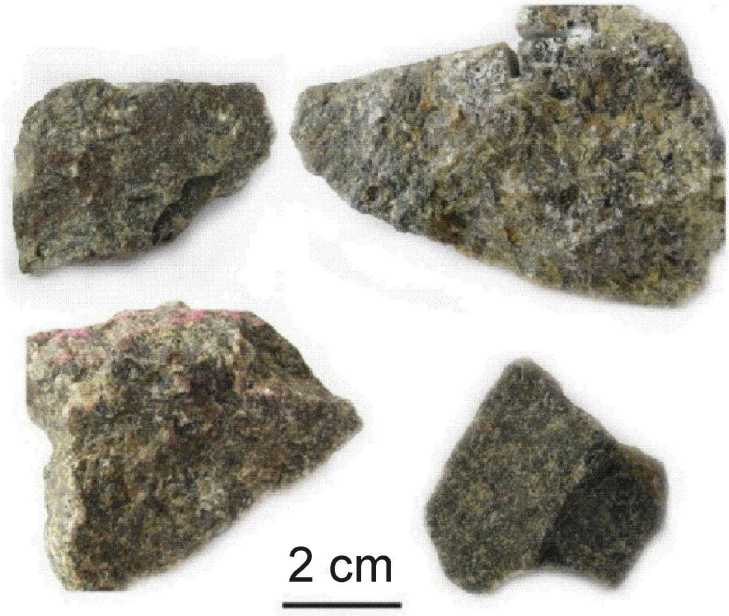

Fig. 2. Enderbites of Haivoronskyi complex.

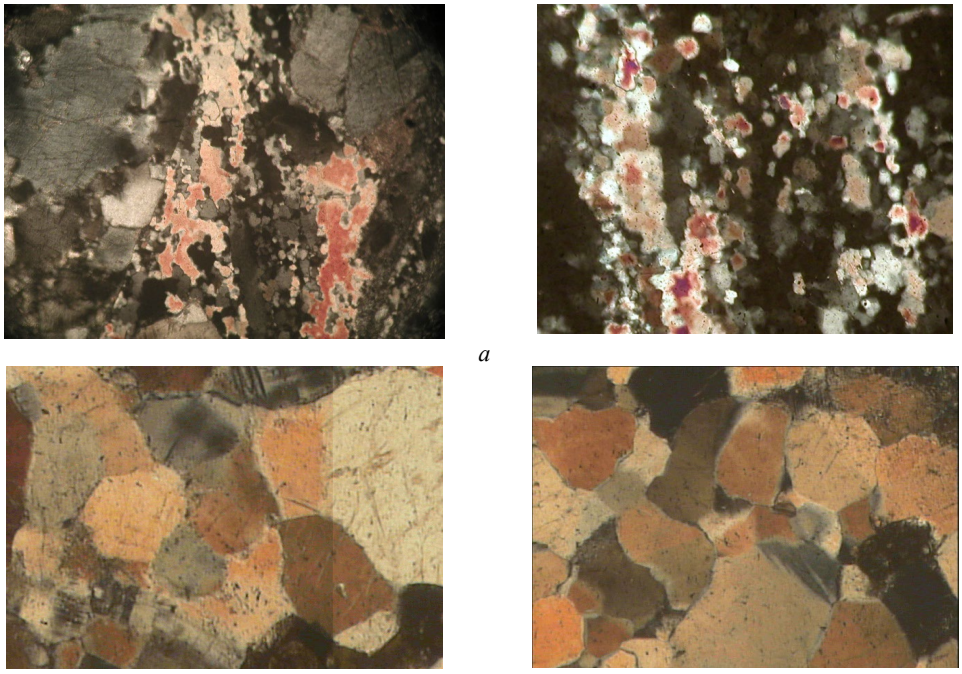

a

b

Fig. 3. Quartz of the first (*a*) and the second (*b*) generations, field of view – 2 mm, cross-polarised light (XPL).

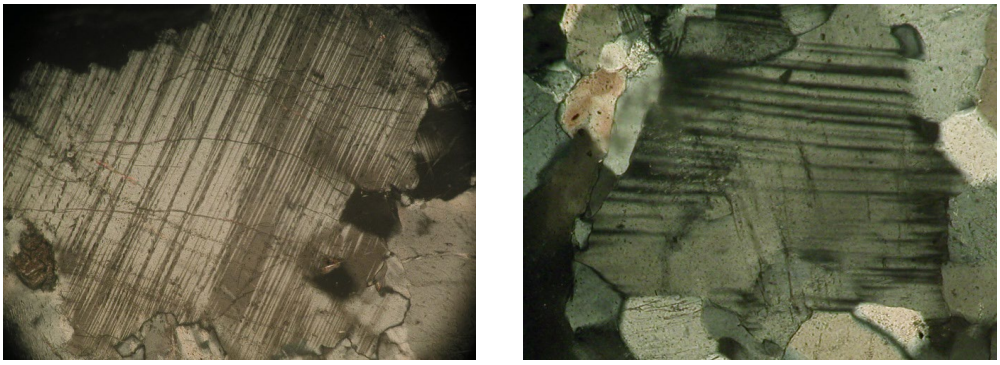

Fig. 4. Polysynthetic twins of plagioclase, field of view – 2 mm, XPL.

Table 1

Chemical composition (wt. %) and formula coefficients of plagioclase from enderbites of the Odeskyi quarry

Components	Sample number				
	4	13	18	19	25
SiO_2	54.20	42.79	63.98	55.76	55.18
TiO_2	0.00	0.00	0.00	0.00	0.00
Al_2O_3	29.93	37.41	22.71	28.39	29.24
FeO	0.20	1.05	0.17	0.00	0.31
MnO	0.30	0.00	0.00	0.00	0.08
MgO	1.36	1.82	1.39	1.23	1.49
CaO	6.39	14.71	5.65	7.38	6.75
Na_2O	7.35	2.19	5.26	7.10	6.63
K_2O	0.27	0.05	0.05	0.14	0.33
Total	100.00	100.02	99.21	100.00	100.01
Formula coefficients					
Si	2.44	1.98	2.82	2.50	2.47
Al	1.56	2.02	1.18	1.50	1.53
Total	4.00	4.00	4.00	4.00	4.00
Ca	0.31	0.73	0.27	0.35	0.32
Na	0.64	0.20	0.45	0.62	0.58
K	0.02	0.00	0.00	0.01	0.02
Total	0.96	0.93	0.72	0.98	0.92
X–(Ab)–Pl	0.66	0.21	0.63	0.63	0.63
X–(An)–Pl	0.32	0.79	0.37	0.36	0.35
X–(Kfs)–Pl	0.02	0.00	0.00	0.01	0.02

Variations in the chemical composition of plagioclases in the three-component K–Na–Ca system are shown in Fig. 5.

Plagioclases of basic and intermediate composition (from bytownite to andesine) are earlier; they form syngenetic boundaries with potassium feldspar (Fig. 6).

Acidic plagioclases (oligoclase–albite) replace earlier plagioclases with the formation of calcite according to the following scheme (albitization process):

$$Ca[Al_2Si_2O_8] + Na^+ + CO_2 \leftrightarrow Na[AlSi_3O_8] + CaCO_3.$$

Table 2

Chemical composition (wt. %) and formula coefficients of plagioclases from enderbites of the Haivoronskyi quarry

Components	Sample and analysis number				
	7.1			1.1	
	3	1	5	7	15
SiO_2	62.81	63.86	62.22	53.18	55.40
Al_2O_3	22.94	22.66	22.18	30.07	29.61
FeO	0.00	0.00	0.00	0.09	0.18
MnO	0.00	0.03	0.00	0.00	0.00
MgO	0.00	0.00	0.00	1.33	1.03
CaO	5.35	4.05	5.21	9.55	7.25
Na_2O	8.53	9.26	8.72	5.56	6.38
K_2O	0.37	0.15	0.34	0.23	0.15
Total	100.00	100.00	98.67	100.01	100.00
Formula coefficients					
Si	2.79	2.82	2.80	2.40	2.48
Al	1.20	1.18	1.18	1.60	1.52
Total	3.98	4.00	3.97	4.00	4.00
Ca	0.25	0.19	0.25	0.46	0.35
Na	0.73	0.79	0.76	0.49	0.55
K	0.02	0.01	0.02	0.01	0.01
Total	1.01	0.99	1.03	0.96	0.91
X–(Ab)–Pl	0.73	0.80	0.74	0.51	0.61
X–(An)–Pl	0.25	0.19	0.24	0.48	0.38
X–(Kfs)–Pl	0.02	0.01	0.02	0.01	0.01

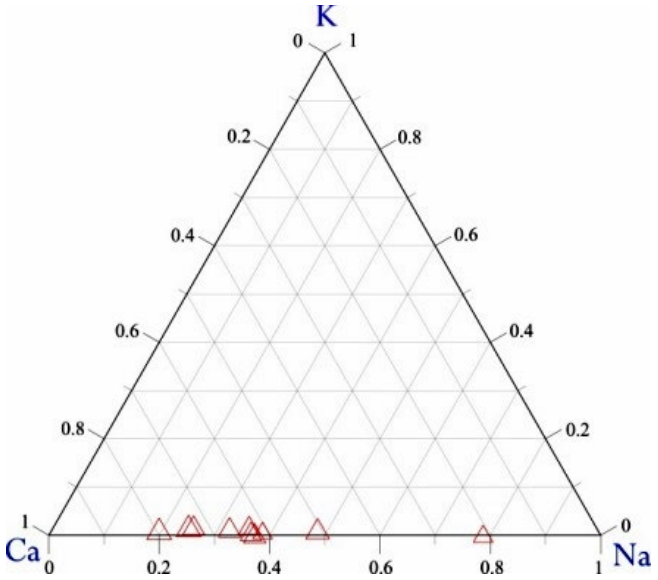

Fig. 5. Variations in the chemical composition of plagioclases in the K–Na–Ca system.

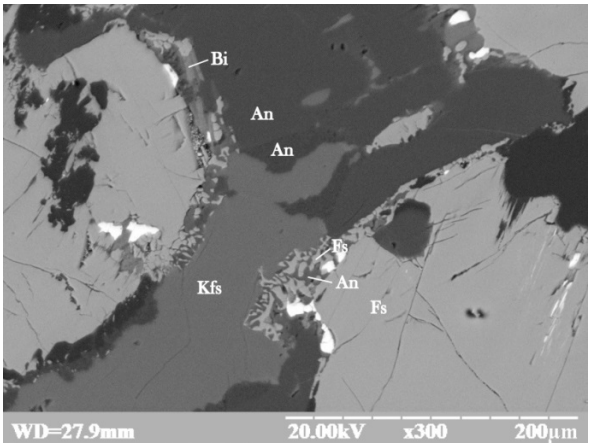

Fig. 6. Syngenetic boundaries of plagioclase with potassium feldspar. An – anorthite, Kfs – potassium feldspar, Bi – biotite, Fs – ferrosilite. BSE image.

Sericite also develops on plagioclase:

$$(Na,Ca)[AlSi_3O_8] + K^+ + H_2O \leftrightarrow (K,Na)Al_2(OH)_2[AlSi_3O_{10}] + Ca^{2+}.$$

Potassium feldspar forms tabular grains 0.2–0.9 mm in size and pinkish in colour. A microcline lattice is visible in translucent light (Fig. 7, *a*); microperthites are characteristic – plagioclase ingrowths in K-feldspar (see Fig. 7, *b*) and microantiperthites – ingrowths of K-feldspar in plagioclase (see Fig. 7, *c*).

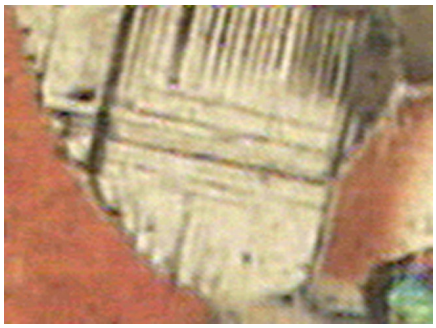

a

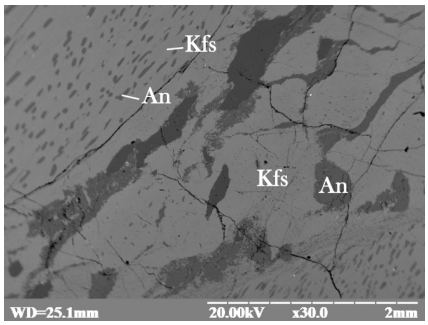

b

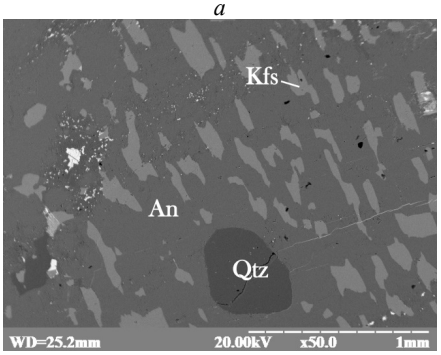

c

Fig. 7. Internal structure of potassium feldspar grains: *a* – microcline lattice, field of view – 2 mm, XPL; *b* – microperthites; *c* – microantiperthites; Qtz – quartz. BSE image.

X-ray analysis was performed to determine the system of potassium feldspar [1]. The triclinicity of the mineral is $\Delta p = 0.79$ (triclinic system); therefore, it is a microcline. The chemical composition of potassium feldspars is given in Table 3.

Table 3

Chemical composition (wt. %) and formula coefficients of potassium feldspars

Components	Sample and analysis number						
	Кяр-9		1.1		7-1		
	5	4	10	14	2	4	6
SiO_2	59.36	58.51	60.28	60.03	64.57	63.75	64.05
TiO_2	0.73	1.26	0.98	0.67	0.00	0.00	0.00
Al_2O_3	21.56	22.33	21.1	22.37	17.99	17.88	18.27
V_2O_3	0.00	0.16	0.00	0.00	0.00	0.00	0.00
FeO	0.00	0.27	1.57	0.03	0.00	0.00	0.00
MnO	0.00	0.00	0.06	0.00	0.00	0.00	0.00
MgO	1.51	1.05	0.97	1.34	0.00	0.00	0.00
BaO	0.00	0.00	0.00	0.00	0.39	0.79	0.58
CaO	0.27	0.34	0.64	0.35	0.33	0.54	0.67
Na_2O	1.87	1.30	0.96	0.93	1.94	1.59	1.96
K_2O	14.70	14.78	13.44	14.28	14.78	15.45	14.47
Total	100.00	100.00	100.00	100.00	100.00	100.00	100.00
Formula coefficients							
Si	2.77	2.73	2.80	2.78	2.99	2.98	2.97
Al	1.18	1.23	1.15	1.22	0.98	0.98	1.00
Ti	0.03	0.04	0.03	0.01	0.00	0.00	0.00
Total	3.98	4.00	3.99	4.00	3.97	3.96	3.97
Ca	0.01	0.02	0.03	0.017	0.02	0.03	0.03
Ba	0.00	0.00	0.00	0.00	0.17	0.01	0.01
Na	0.17	0.12	0.09	0.083	0.01	0.14	0.18
K	0.87	0.88	0.80	0.842	0.87	0.92	0.86
Total	1.06	1.01	0.91	0.94	1.07	1.11	1.08
X–(Ab)–Kfs	0.83	0.87	0.87	0.89	0.97	0.84	0.80
X–(An)–Kfs	0.16	0.12	0.09	0.09	0.01	0.13	0.17
X–(Or)–Kfs	0.01	0.02	0.04	0.02	0.02	0.02	0.03

Potassium feldspar develops on compressed plagioclase of intermediate to basic composition (labradorite–bytownite) (Fig. 8).

Among the *pyroxenes*, rhombic (ferrosilite) and monoclinic (diopside, augite) pyroxenes were found. Ferrosilite forms short-prismatic grains ranging in size from 0.1 to 0.4–1.0 mm, dark green, colourless in translucent light (Fig. 9), the grains are deformed and fractured (Fig. 10). Ferrosilite and diopside form syngenetic growths (Fig. 11). Monoclinic pyroxenes are represented by prismatic grains ranging in size from 0.1–0.3 to 1 mm. The chemical composition of pyroxenes is given in Table 4 and depicted on the Ca–Fe–Mg triangular diagram (Fig. 12).

Garnet forms porphyroblasts ranging in size from 0.2–1.0 to 5 mm or more (Fig. 13), develops on a plagioclase-pyroxene aggregate (Fig. 14, *a*) and forms syngenetic growths with biotite (see Fig. 14, *b*).

Garnet grains contain segregations of quartz, ilmenite, calcite; garnet and quartz formed simultaneously.

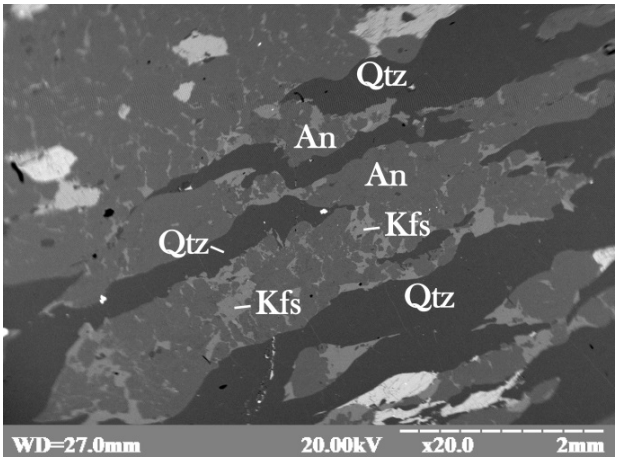

Fig. 8. Development of potassium feldspar on compressed plagioclase. BSE image.

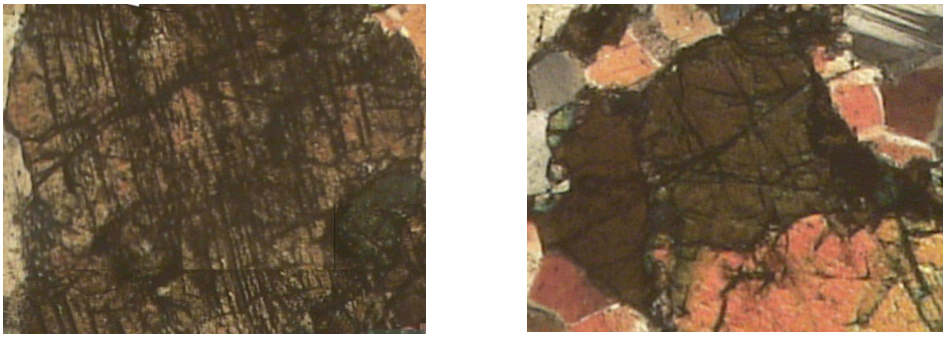

Fig. 9. Grains of rhombic pyroxene in enderbite, field of view – 2 mm, XPL.

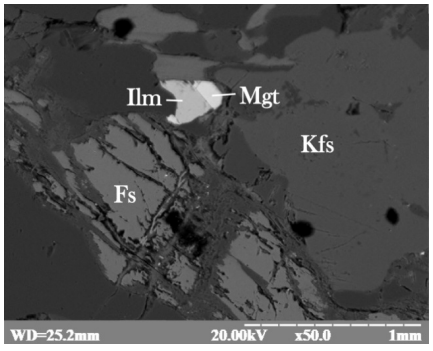

Fig. 10. Fractured orthopyroxene (Fs), as well as ilmenite (Ilm), magnetite (Mgt), and K-spar in enderbite. BSE image.

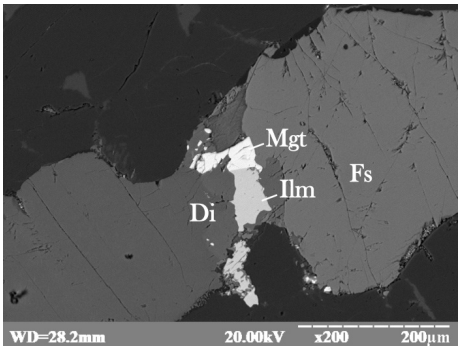

Fig. 11. Syngenetic growths of diopside (Di) and ferrosilite, along which magnetite develops. BSE image.

The chemical composition of garnets from enderbites is given in Table 5 and shown in Fig. 15.

Table 4

Chemical composition (wt. %) and formula coefficients of rhombic (*1–9*) and monoclinic (*10–14*) pyroxenes from enderbites

Components	Sample and analysis number						
	Кяр 9						5a
	11	16	24	27	29	35	1
	1	*2*	*3*	*4*	*5*	*6*	*7*
SiO_2	46.86	46.26	46.43	45.76	46.11	46.53	41.63
TiO_2	0.12	0.09	0.00	0.00	0.00	0.18	0.16
Al_2O_3	2.68	3.85	3.12	2.60	6.06	2.93	1.63
V_2O_3	0.00	0.00	0.18	0.00	0.21	0.00	0.00
Cr_2O_3	0.00	0.00	0.08	0.00	0.00	0.00	0.00
Fe_2O_3	0.44	0.00	0.13	1.49	0.00	0.46	4.27
FeO	32.58	34.40	35.56	35.88	28.91	34.36	44.01
MnO	0.50	0.48	0.74	0.41	0.66	0.50	0.31
MgO	15.68	14.24	13.75	13.86	14.95	14.40	7.99
CaO	0.58	0.34	0.00	0.00	1.65	0.64	0.00
Na_2O	0.46	0.32	0.00	0.00	1.27	0.00	0.00
K_2O	0.10	0.01	0.00	0.00	0.18	0.00	0.00
Total	100.00	100.00	100.00	100.00	100.00	100.00	100.00
Formula coefficients							
Si	1.86	1.84	1.86	1.85	1.80	1.86	1.78
Al	0.13	0.16	0.15	0.12	0.28	0.14	0.08
Ti	0.00	0.00	0.00	0.00	0.00	0.00	0.01
Fe^{3+}	0.01	0.00	0.00	0.05	0.00	0.01	0.14
Total	2.00	2.00	2.00	2.00	2.00	2.00	2.01
Al	0.00	0.02	0.00	0.00	0.00	0.00	0.00
Fe^{2+}	1.08	1.15	1.19	1.21	0.95	1.15	1.58
Mg	0.93	0.85	0.82	0.83	0.87	0.86	0.51
Mn	0.02	0.02	0.03	0.01	0.02	0.02	0.01
Total	2.02	2.03	2.04	2.06	1.84	2.02	2.10
Fe/(Fe+Mg)	0.54	0.58	0.59	0.60	0.52	0.58	0.77
Mg/(Fe+Mg)	0.46	0.42	0.41	0.40	0.48	0.42	0.23

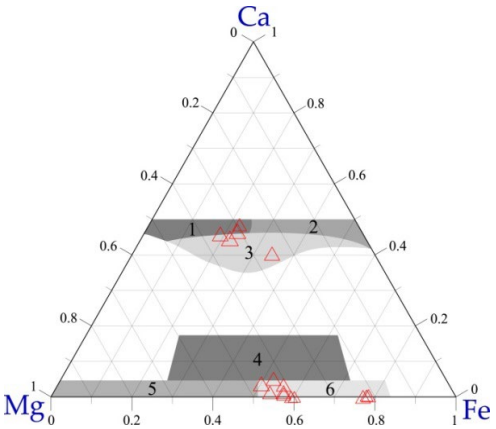

Fig. 12. Variations in the chemical composition of pyroxenes in the Ca–Fe–Mg system.

End of the Table 4

Components	Sample and analysis number						
	5a		Кяр 9		1-1		
	4	7	10	34	6	11	12
	8	*9*	*10*	*11*	*12*	*13*	*145*
SiO_2	42.71	42.29	47.58	48.01	50.30	49.40	41.28
TiO_2	0.00	0.10	0.03	0.00	0.00	0.00	9.08
Al_2O_3	1.59	1.62	4.37	3.35	2.92	3.37	2.74
V_2O_3	0.00	0.00	0.21	0.00	0.00	0.00	0.00
Cr_2O_3	0.00	0.00	0.00	0.25	0.00	0.00	0.00
Fe_2O_3	2.95	3.32					
FeO	44.48	44.43	13.77	11.92	13.53	13.82	20.15
MnO	0.73	0.52	0.24	0.00	0.29	0.00	0.00
MgO	7.24	7.48	11.84	12.52	9.92	10.44	8.29
CaO	0.14	0.16	21.94	22.66	22.93	22.08	18.44
Na_2O	0.00	0.00	0.00	1.22	0.06	0.88	0.00
K_2O	0.14	0.07	0.00	0.06	0.05	0.01	0.02
Total	100.00	100.00	100.00	100.00	100.00	100.00	100.00
Formula coefficients							
Si	1.82	1.81	1.83	1.84	1.93	1.90	1.65
Al	0.08	0.08	0.17	0.15	0.08	0.11	0.13
Ti	0.00	0.00	0.00	0.00	0.00	0.00	0.22
Fe^{3+}	0.09	0.11					
Total	2.00	2.00	2.00	1.99	2.00	2.00	2.00
Al	0.00	0.00	0.03	0.00	0.06	0.05	0.00
Ti			0.00	0.00	0.00	0.00	0.05
Fe^{2+}	1.59	1.59	0.44	0.38	0.43	0.44	0.67
Mg	0.46	0.48	0.68	0.72	0.57	0.60	0.49
Mn	0.03	0.02	0.01	0.00	0.01	0.00	0.00
V			0.01	0.01	0.00	0.00	0.00
Total	2.08	2.08	1.16	1.11	1.07	1.09	1.22
Ca			0.90	0.93	0.94	0.91	0.79
Na			0.00	0.09	0.01	0.07	0.00
Total			0.90	1.02	0.95	0.97	0.79
Fe/(Fe+Mg)	0.79	0.78	0.39	0.35	0.57	0.57	0.42
Mg/(Fe+Mg)	0.21	0.22	0.61	0.65	0.43	0.43	0.58

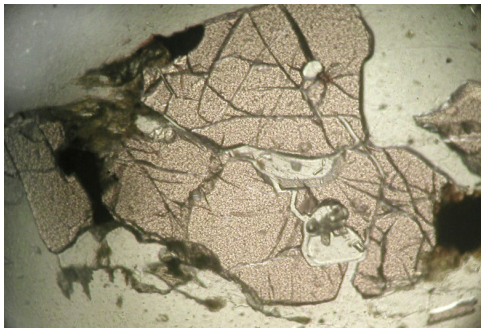

Fig. 13. Porphyroblast of garnet, field of view – 2 mm, plane-polarised light (PPL).

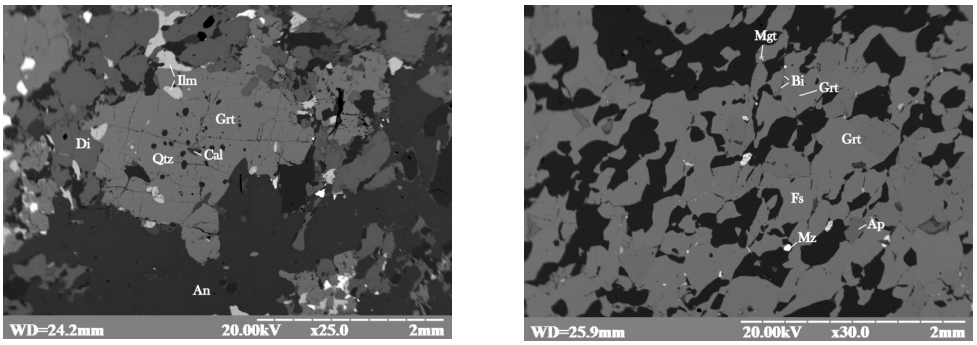

a *b*

Fig. 14. Development of garnet on the plagioclase-pyroxene aggregate (*a*) and syngenetic growths of garnet with biotite (*b*). Grt – garnet, An – plagioclase, Cal – calcite, Mz – monazite, Ar – apatite. BSE image.

Table 5

Chemical composition (wt. %) and formula coefficients of garnets from enderbites

Components	Sample and analysis number					
	1.1				5a	
	1	2	8	9	2	3
SiO_2	35.64	36.35	35.85	36.02	32.16	33.04
TiO_2	0.00	0.00	0.00	0.00	0.11	0.00
Al_2O_3	22.00	21.38	21.24	22.02	20.62	20.97
Fe_2O_3	1.62	1.49	2.92	1.43	4.30	3.08
FeO	28.72	28.82	28.26	28.69	36.22	36.98
MnO	1.08	0.98	0.85	1.00	2.70	2.31
MgO	3.40	3.52	3.74	2.51	2.35	1.91
CaO	7.53	7.46	7.03	8.21	1.41	1.65
Na_2O	0.00	0.00	0.00	0.12	0.00	0.00
K_2O	0.00	0.00	0.10	0.00	0.13	0.06
Total	100.00	100.00	100.00	100.00	100.00	100.00
Formula coefficients						
Si	2.85	2.90	2.87	2.88	2.69	2.75
Al	0.15	0.10	0.13	0.12	0.31	0.25
Total	3.00	3.00	3.00	3.00	3.00	3.00
Al	1.92	1.91	1.87	1.96	1.72	1.81
Ti	0.00	0.00	0.00	0.00	0.01	0.00
Fe^{3+}	0.10	0.09	0.18	0.09	0.27	0.19
Total	2.02	2.00	2.04	2.04	2.00	2.00
Fe^{2+}	1.92	1.92	1.89	1.92	2.53	2.57
Mg	0.41	0.42	0.45	0.30	0.29	0.24
Mn	0.07	0.07	0.06	0.07	0.19	0.16
Ca	0.65	0.64	0.60	0.70	0.13	0.15
Total	3.04	3.05	3.00	2.99	3.16	3.12
Almandine	0.63	0.63	0.63	0.64	0.81	0.82
Pyrope	0.13	0.14	0.15	0.10	0.09	0.08
Spessartine	0.02	0.02	0.02	0.02	0.06	0.05
Grossular	0.21	0.21	0.20	0.24	0.04	0.05

Biotite in transparent sections is pale yellow with its characteristic pleochroism scheme; grains have a scaly shape and size from 0.2–0.6 to 1 mm (Fig. 16). The mineral forms syngenetic growths with garnet (see Fig. 14, *b*), as well as with monazite, forming an induction surface. Chemical composition and formula coefficients of biotite see in the Table 6.

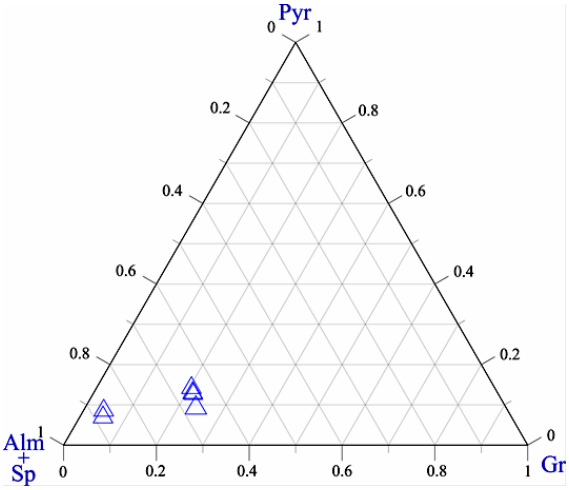

Fig. 15. Variations in the chemical composition of garnet in the three-component system Pyr–Gr–(Alm+Sp).

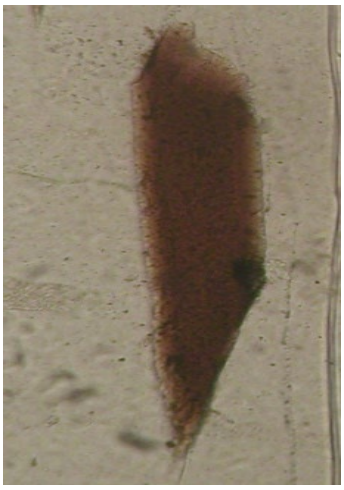

Fig. 16. Grain of biotite, field of view – 2 mm, PPL.

Apatite is visible only under a microscope: it is represented by separate isometric grains of 0.05–0.25 mm in size and growths with monazite (Fig. 17).

Ilmenite is also visible only in sections – these are individual grains of irregular shape 0.1–0.4 mm in size and growths with magnetite (see Fig. 17, *a*). The chemical composition and formula coefficients of ilmenite are given in the Table 7.

Monazite, detected by microprobe analysis, forms isometrically shaped grains 0.1–0.4 mm in size and growths with biotite (see Fig. 17, *a*). The chemical composition of monazite is as follows, wt. %: P_2O_5 – 35,60; Ce_2O_3 – 33,50; La_2O_3 – 15,94; Nd_2O_3 – 7,24; Pr_2O_3 – 5,65; CaO – 2,08. The crystal chemical formula of the mineral is as follows:

$$(Ce_{0.44}La_{0.21}Nd_{0.09}Ca_{0.08}Pr_{0.07})_{0.89}[P_{1.08}O_4].$$

Magnetite, detected by microprobe analysis, is represented by isometric and irregularly shaped grains in growths with ilmenite (see Fig. 17, *a*). The chemical composition and formula coefficients of magnetite are given in the Table 8.

Carbonates, according to the results of microprobe analysis, are represented by calcite and dolomite (Table 9), which form inclusions in the garnet with a size of 0.2–0.6 mm (see Fig. 14, *a* and 18).

Determination of the temperature of mineral formation using mineral geothermometers. To determine the temperature of mineralization, we used biotite-garnet, garnet-orthopyroxene, and two-feldspar (plagioclase-K-feldspar) geothermometers.

To determine the temperature using a *garnet-biotite geothermometer*, a sample was selected in which garnet and biotite in enderbite form syngenetic growths.

The following two garnet–biotite mineral pairs were chosen:

Table 6

Chemical composition (wt. %) and formula coefficients of biotite from enderbites

Components	Sample and analysis number						
	Кяр-9					5a	
	2	17	20	22	28	5	6
SiO_2	35.44	36.54	35.55	35.55	34.68	32.58	33.92
TiO_2	1.93	0.24	0.15	0.15	6.13	4.79	5.01
Al_2O_3	18.13	21.22	19.48	19.48	16.77	15.58	14.62
FeO	20.04	17.62	19.93	19.93	20.34	29.40	28.45
MnO	0.00	0.00	0.00	0.00	0.00	0.06	0.00
MgO	12.74	12.03	14.44	14.44	10.47	6.10	6.98
CaO	0.38	1.31	0.43	0.43	0.65	0.40	0.21
Na_2O	0.65	0.89	0.56	0.56	0.57	0.38	0.40
K_2O	10.69	10.14	9.47	9.47	10.40	10.70	10.41
Total	100.00	100.00	100.00	100.00	100.00	100.00	100.00
Formula coefficients							
Si	2.61	2.64	2.59	2.65	2.56	2.54	2.62
Al	1.39	1.36	1.41	1.35	1.44	1.43	1.33
Ti	0.00	0.00	0.00	0.00	0.00	0.03	0.06
Total	4.00	4.00	4.00	4.00	4.00	4.00	4.00
Al	0.18	0.44	0.26	0.30	0.01	0.00	0.00
Ti	0.11	0.01	0.01	0.00	0.34	0.25	0.23
Fe	1.23	1.06	1.21	1.11	1.25	1.91	1.83
Mg	1.40	1.29	1.57	1.54	1.15	0.71	0.80
Total	2.92	2.82	3.05	2.96	2.76	2.87	2.87
Ca	0.03	0.10	0.03	0.05	0.05	0.03	0.02
Na	0.09	0.12	0.08	0.11	0.08	0.06	0.06
K	1.00	0.93	0.88	0.92	0.98	1.06	1.02
Total	1.13	1.16	0.99	1.08	1.11	1.15	1.10
Fe/(Fe+Mg)	0.47	0.45	0.44	0.42	0.52	0.73	0.70
Mg/(Fe+Mg)	0.53	0.55	0.56	0.58	0.48	0.27	0.30

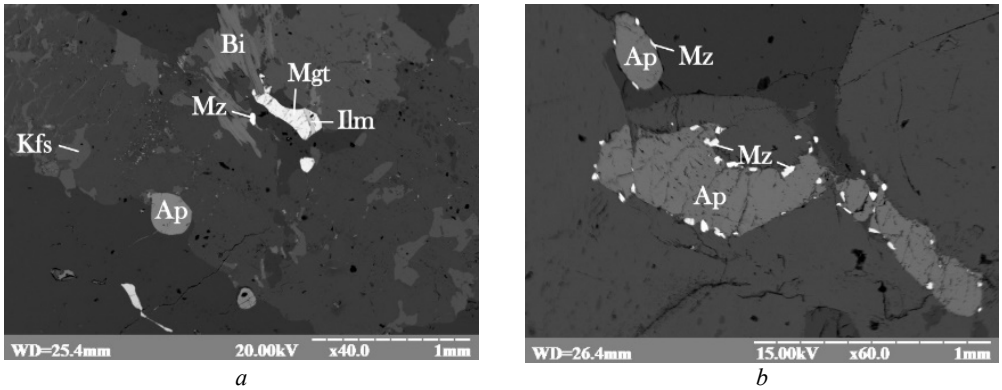

a *b*

Fig. 17. Isometric apatite grain, growths of ilmenite (*a*) and apatite with monazite (*b*).
BSE image.

Table 7

Chemical composition (wt. %) and formula coefficients of ilmenite from enderbites

Components	Analysis number (sample Кяр-9)			
	6	6a	9	30
TiO_2	50.85	49.59	48.82	48.96
Al_2O_3	0.49	0.48	0.95	0.85
V_2O_3	0.00	1.56	1.23	1.94
Fe_2O_3	0.00	0.00	0.00	2.16
FeO	47.92	47.60	47.94	45.60
MnO	0.17	0.51	0.21	0.00
MgO	0.56	0.56	0.56	0.48
Total	100.00	100.00	100.00	100.00
Formula coefficients				
Fe^{2+}	1.02	0.99	1.01	0.98
Mg	0.02	0.02	0.02	0.02
Mn	0.00	0.00	0.01	0.00
Total	1.04	1.01	1.04	1.00
Ti	0.97	0.93	0.92	0.93
V	0.00	0.03	0.02	0.04
Fe^{3+}	0.00	0.00	0.00	0.02
Al	0.01	0.01	0.03	0.03
Total	0.98	0.97	0.97	1.02

Table 8

Chemical composition (wt. %) and formula coefficients of magnetite from enderbites

Components	Analysis number (sample Кяр-9)		
	7	8	31
TiO_2	0.46	0.46	0.01
Al_2O_3	0.78	1.08	1.61
V_2O_3	1.86	1.37	2.85
Cr_2O_3	3.70	2.21	4.16
Fe_2O_3	60.82	63.44	59.82
FeO	31.86	30.98	30.63
MnO	0.51	0.32	0.72
MgO	0.00	0.14	0.19
Total	100.00	100.00	100.00
Formula coefficients			
Fe^{2+}	1.01	0.98	0.97
Mg	0.00	0.01	0.01
Mn	0.02	0.01	0.02
Total	1.03	1.00	1.00
Fe^{3+}	1.74	1.81	1.71
Al	0.04	0.05	0.07
Ti	0.01	0.01	0.00
V	0.06	0.04	0.09
Cr	0.11	0.07	0.13
Total	1.96	1.98	2.00

Table 9

Chemical composition (wt. %) and formula coefficients of carbonates from enderbites

Components	Analysis number (sample 1.1)		
	3	4	13
FeO	12.91	9.48	11.78
MgO	10.96	13.36	12.24
MnO	0.33	0.47	0
CaO	29.34	29.06	28.06
Total	53.54	52.37	52.08
Formula coefficients			
Ca	0.53	0.52	1.03
Mg	0.28	0.34	0.63
Mn	0.01	0.01	0.00
Fe	0.18	0.13	0.34
Total	1.00	1.00	2.00

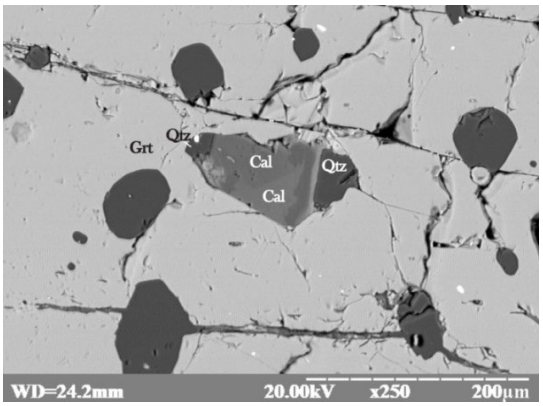

Fig. 18. Inclusions of calcite and quartz in garnet. BSE image.

$Alm_{0.81}Pyr_{0.09}Sp_{0.06}Gr_{0.04} – (K_{1.06}Na_{0.05}Ca_{0.03})(Fe_{1.90}Mg_{0.70}Ti_{0.24}Mn_{0.003})[Al_{1.4}Si_{2.5}O_{10}](OH)_2$

(See analysis No. 2 (sample 5a) in Table 5 – analysis No. 5 in Table 6);

$Alm_{0.82}Pyr_{0.08}Sp_{0.05}Gr_{0.05} – (K_{1.02}Na_{0.05}Ca_{0.01})(Fe_{1.83}Mg_{0.80}Ti_{0.23})[Al_{1.32}Si_{2.61}O_{10}](OH)_2$

(See analysis No. 3 in Table 5 – analysis No. 6 in Table 6).

Two methods were used – based in theoretical calculations and a graphic method. The obtained values of the temperature of mineral formation based on theoretical calculations accorging to the data of various authors are given in the Table 10, and accorfing to the graphic method – in Fig. 19 (600–650 °C).

To determine the temperature using the *garnet-orthopyroxene geothermometer*, we selected a sample in which garnet and orthopyroxene form syngenetic growths. One mineral pair was used:

$Alm_{0.8}\ Pyr_{00.9}\ Sp_{0.06}\ Gr_{0.04} – (Fe_{1.57}Mg_{0.51}Mn_{0.01})[Si_{1.78}Fe_{0.13}Al_{0.08}Ti_{0.05}O_6]$

(See analysis No. 2 in Table 5 – analysis No. 1 in Table 4).

According to various authors (see Table 10), the temperature of mineral formation ranges from 415 to 481 °C.

Table 10

The results of determining the temperature of mineral formation based on the calculation method using biotite-garnet, garnet-orthopyroxene and two-feldspar geothermometers according to the data of various authors

Geothermometer	Authors	Temperature, °C
Biotite-garnet	Goldman, Albee [15]	649–556
	Lavrent'eva, Perchuk [2]	719–630
	Holdaway, Lee [18]	728–616
	Thompson [26]	767–635
	Ferry, Spear [13]	821–636
	Perchuk, Lavrent'eva [22]	660–609
		721–624
		721–632
Garnet-orthopyroxene	Harley [17]	415
	Bhattacharya et al. [12]	418
	Perchuk [21]	451
	Lee, Ganguly [19]	481
Two-feldspar	Powell, Powell [23]	516
	Furhman, Lindsley [14]	519
	Green, Usdansky [16]	526
	Perchuk et al. [20]	529
	Stormer [24]	531
	Stormer, Whitney [25]	577

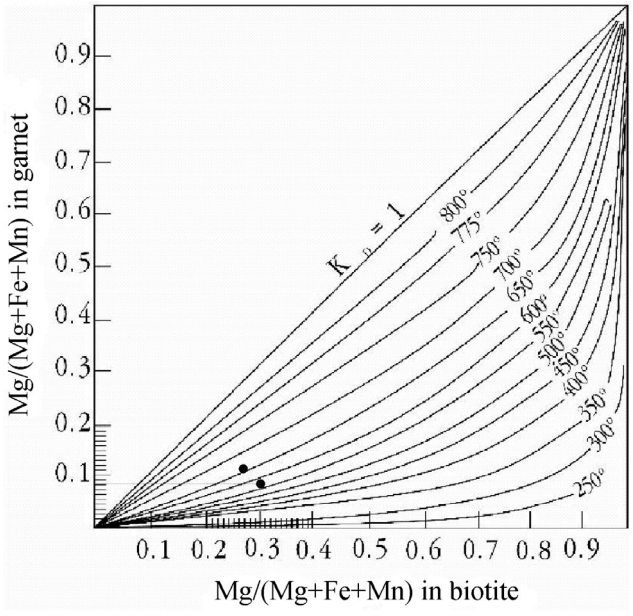

Fig. 19. Results of determining the temperature of mineral formation (black dots) using a biotite-garnet geothermometer. Mg and Fe distribution isotherms between biotite (Bi) and garnet (Gr) are shown [5].

To determine the temperature using a *two-feldspar geothermometer*, we chose the mineral pair plagioclase–potassium feldspar (the minerals form a syngenetic growth): $Ab_{0.66}An_{0.32}Kf_{0.02}$–$Kf_{0.83}Ab_{0.16}An_{0.01}$. According to the data of various authors, the determined value of the temperature of the mineral formation ranges from 516 to 577 °C (see Table 10).

Conclusions. The conducted research made it possible to determine the mineralogical and petrographic features and conditions of formation of enderbites of the Haivoron complex in the area of the urban-type village of Zavallia.

Enderbites are massive medium-coarse-grained grey, dark grey, greenish-grey rocks with a grano- or heteroblastic structure. The mineral composition of enderbites includes quartz, plagioclase, K-feldspar, pyroxenes, garnet, biotite, hornblende, accessory minerals are represented by apatite, zircon, titanite, monazite, calcite, dolomite, and ore minerals – by ilmenite, pyrite, magnetite.

Two generations of quartz are distinguished: early quartz is represented by elongated grains with stylolitic boundaries in contact with other minerals; late quartz in the form of isometric grains with wavy extinction has been formed as a result of recrystallization. Plagioclase of the first generation has a composition from bytownite to andesine ($An_{0.79–0.32}$) and forms perthite and antiperthite ingrowths; plagioclases of the second generation are represented by oligoclase ($An_{0.25–0.19}$), they replace earlier plagioclase with the formation of calcite. Potassium feldspar replaces plagioclase with the appearance of antiperthite ingrowths and is represented by microcline. Garnet forms porphyroblasts and syngenetic growths with biotite, and magnetite forms syngenetic growths with ilmenite, which indicates the simultaneous formation of these minerals. Apatite develops in shatter zones and forms syngenetic growths with monazite and xenotime.

Our research and available literature data [4] provide grounds for distinguishing several stages in the process of enderbite formation.

The first, earliest stage is the stage of transition from original rocks to antiperthite enderbites. It is associated with intensive recrystallization, alkaline metasomatosis (with a predominant sodium value) and silicic metasomatosis: the general enrichment of newly formed rocks with plagioclase of a more acidic composition compared to the plagioclase of the original rocks, and the appearance of biotite and a small amount of K-spar in the form of antiperthite ingrowths.

The second stage is the stage of formation of antiperthitic enderbites enriched in quartz; recrystallization of rocks and intense silicic metasomatosis continued. Alkaline metasomatosis in this case has a subordinate value. There is a general enrichment of the rock with quartz, replacement of coloured minerals with plagioclase, formation of antiperthite ingrowths and biotite. These processes occurred during the first stage of substrate melting (3.65–3.40 billion years) [11].

The third stage, the latest one, is the stage of charnockite formation. It is also associated with recrystallization and alkaline metasomatosis (a greater amount of potassium compared to sodium, which led to the formation of potassium feldspar). During the growth of K-spar grains, solutions were depleted of potassium and enriched with sodium and calcium, which led to the formation of myrmekites and perthite ingrowths in K-spar at the end of the stage. A garnet-biotite paragenesis is formed, which is superimposed and associated with high-temperature solutions (T = 609–821 °C according to the garnet-biotite geothermometer); these solutions brought Al, Fe, Ba, and K into the system. Metasomatosis was syntectonic during

the second stage of melting of the substrate (2.78–2.74 billion years ago) and the formation of charnockites [6].

REFERENCES

1. Giller, Ya. L. (1966). *Tables of interplanar distances.* Moscow: Nedra. (in russian)
2. Larent'eva, I. V., & Perchuk, L. L. (1981). Phase correspondence in the biotite–garnet system. Experimental data. *Reports of the Academy of Sciences of the USSR, 260 (3),* 731–734. (in russian)
3. Lesnaia, I. M. (1988). *Geochronology of charnockites of Pobuzhie.* Kiev: Naukova dumka. (in russian)
4. Nalivkina, E. B. (1977). *Ophiolite associations of the Early Precambrian of Ukraine.* Moscow: Nedra. (in russian)
5. Perchuk, L. L. (1967). Biotite-garnet geothermometer. *Reports of the Academy of Sciences of the USSR, 177 (2),* 111–114. (in russian)
6. Semenenko, N. P. (1995). *Granulites and charnockites of the Ukrainian Shield.* Kiev: Naukova dumka. (in russian)
7. Usenko, I. S. (1958). *Basic and ultrabasic rocks of the Southern Bug basin.* Kiev: Publishing House of the Academy of Sciences of the Ukrainian SSR. (in russian)
8. Usenko, I. S. (Ed.). (1985). *Granulitic facies of the Ukrainian Shield.* Kiev: Naukova dumka. (in russian)
9. Shcherbak, N. P. (Ed.). (1984). *Granitoid formations of the Ukrainian Shield.* Kiev: Naukova dumka. (in russian)
10. Shcherbak, N. P., Artemenko, G. V., Lesnaia, G. V., & Ponomarenko, A. N. (2005). *Geochronology of the Early Precambrian of the Ukrainian Shield. Archean.* Kiev: Naukova dumka. (in russian)
11. Shcherbakov, I. B. (2005). *Petrology of the Ukrainian Shield.* Lvov: ZUKC. (in russian)
12. Bhattacharya, A., Mohanty, L., Maji, A., Sen, S. K., & Raith, M. (1992). Non-ideal mixing in the phlogopite–annite boundary: constraint from experimental data on Fe–Mg partitioning and reformulation of the biotite–garnet geothermometer. *Contrib. Mineral. Petrol., 111,* 87–93.
13. Ferry, J. M., & Spear, F. S. (1978). Experimental calibration of the partitioning of Fe and Mg between biotite and garnet. *Contrib. Mineral. Petrol., 66,* 113–117.
14. Furhman, M. L., & Lindsley, D. H. (1988). Ternary feldspar modeling and thermometry. *Amer. Mineral., 73,* 201–216.
15. Goldman, D. S. Y., & Albee, A. L. (1977). Correlation of Mg/Fe partitioning between garnet and biotite with $^{18}O/^{16}O$ partitioning between quartz and magnetite. *Amer. J. Sci. 277,* 750–767.
16. Green, N. L., & Usdansky, S. I. (1986). Ternary feldspar mixing relations and thermobarometry. *Amer. Mineral., 71,* 1100-8.
17. Harley, S. (1988). Granulite P-T paths: Constraints and implications for granulite genesis. *Terra Cognita, 8,* 267–268.
18. Holdaway, M. J. & Lee, S. M. (1977). Fe-Mg cordierite stability in high-grade pelitic rocks based experimental, theoretical, and natural observations. *Contrib. Mineral. Petrol., 63,* 175–198.

19. Lee, H. Y., & Ganguly, J. (1988). Equilibrium compositions of coexisting garnet and orthopyroxene: Reversed experimental determinations in the system FeO–MgO–Al_2O_3–SiO_2, and applications. *J. Petrol., 29 (1),* 93–113. doi:10.1093/petrology/29.1.93
20. Perchuk L., Gerya, T., & Nozhkin, A. (1989). Petrology and retrograde P-T path in granulites of the Kanskaya formation, Yenisey range, Eastern Siberia. *J. Metamorphic Geol., 7 (6),* 599–617. https://doi.org/10.1111/j.1525-1314.1989.tb00621.x
21. Perchuk, L. L. (1991). Derivation of a thermodynamically consistent set of geothermometers and barometers for metamorphic and magmatic rocks. In L. L. Perchuk (Ed.). *Progress in metamorphic and magmatic petrology.* Cambridge University Press, 93–111.
22. Perchuk, L. L., & Larent'eva, I. V. (1983). Experimental investigation of exchange equilibria in the system cordierite–garnet–biotite. In S. K. Saxena (Ed.). *Kinetics and equilibrium in mineral reactions (Advances in physical geochemistry series, 3).* New York: Springer, 199–239.
23. Powell, R. & Powell, M. (1977). Geothermometry and oxygen barometry using coexisting iron-titanium oxides: a reappraisal. *Mineral. Mag., 41 (318),* 257–263.
24. Stormer, J. C., Jr. (1975). A practical two-feldspar geothermometer. *Amer. Mineral., 60,* 667–674.
25. Stormer, J. C., Jr., & Whitney, J. A. (1985). Two feldspar and iron-titanium oxide equilibria in silicic magmas and the depth of origin of large volume ash-flow tuffs. *Amer. Mineral., 70,* 52–64.
26. Thompson, A. B., (1976). Mineral reactions in pelitic rocks: II. Calculation of some P–T–X (Fe-Mg) phase relations. *Am. J. Sci., 276,* 425–454.

Стаття: надійшла до редакції 16.06.2022
прийнята до друку 29.08.2022

Наталія Білик, Ірина Побережська,
Леонід Скакун, Євгенія Сливко

Львівський національний університет імені Івана Франка,
вул. Грушевського, 4, Львів, Україна, 79005
nataliya.bilyk@lnu.edu.ua

ОСОБЛИВОСТІ РЕЧОВИННОГО СКЛАДУ І ТЕРМОДИНАМІЧНІ УМОВИ ФОРМУВАННЯ ЕНДЕРБІТІВ ГАЙВОРОНСЬКОГО КОМПЛЕКСУ (ПІВДЕННИЙ ЗАХІД УКРАЇНСЬКОГО ЩИТА)

Досліджено мінералого-петрографічні особливості ендербітів гайворонського комплексу в південно-західній частині Українського щита (долина р. Південний Буг від м. Гайворон до смт Завалля). Комплекс досліджень охоплював польові геологічні спостереження на відслоненнях і в кар'єрах та лабораторні петрографічні, мінералогічні й петрогеохімічні дослідження.

Ендербіти – масивні середньо-крупнозернисті породи грано- або гетеробластової структури. Вони містять такі мінерали, як кварц, плагіоклази (альбіт–олігоклаз, андезин–бітовніт), калішпат (мікроклін), ромбічний (феросиліт) і моноклінні (діопсид, авгіт) піро-

ксени, гранати, біотит, апатит, монацит, ільменіт, пірит, гематит, карбонати (кальцит, доломіт). Виділено дві генерації плагіоклазу і кварцу.

За гранат-біотитовим, гранат-ортопіроксеновим і двопольовошпатовим геотермометрами за даними різних авторів з використанням теоретичних розрахунків і графічного методу обчислено температуру мінералоутворення. На підставі виконаних досліджень і літературних даних визначено термодинамічні умови формування ендербітів протягом трьох стадій.

Ключові слова: ендербіти, мінералогія, петрографія, мінералогічні геотермометри, докембрій, Український щит.